Two Schiff-base complexes of cadmium and manganese on modified MCM-41 as practical, recyclable and selective nanocatalysts for the synthesis of sulfoxides

Arida Jabbari[1] · Mohsen Nikoorazm[2] · Parisa Moradi[2]

Abstract

In this work, 2-Hydroxy-5-nitrobenzaldehyde Schiff-base complexes of cadmium and manganese on MCM-41 (Cd-5NSA-MCM-41 and Mn-5NSA-MCM-41) have been investigated as stable, efficient, environment friendly, reusable, and chemoselective nanocatalysts. These catalysts were characterized by various techniques such as X-ray diffraction (XRD), thermogravimetric analysis (TGA), Brunauer–Emmett–Teller (BET), Fourier transform-infrared spectroscopy (FT-IR) and atomic absorption spectroscopy (AAS). Sulfoxide derivatives were synthesized in the presence of Cd-5NSA-MCM-41 and Mn-5NSA-MCM-41 through mild and selective oxidation of sulfides and all sulfoxide products were obtained in good yields within acceptable times. In order to synthesis of sulfoxides, hydrogen peroxide (H_2O_2) was used as an environmentally friendly, non-toxic, available and inexpensive oxidant. These catalysts can recovered and reused for several times without significant loss in catalytic activities. In addition the recovered catalysts was characterized with several techniques such as XRD diffraction, AAS analysis and FT-IR spectroscopy, which are shown a good agreement to fresh catalysts. Comparison of reused and un-reused catalysts were confirmed the heterogeneous nature and good stability of these catalysts.

1 Introduction

Heterogeneous catalytic systems have important materials in green chemistry, organic synthesis and industrial processes [1]. Homogeneous catalysts have excellent activity and selectivity, but they have limited by several drawbacks such as non-reusability and time-consuming of products purification [2–4]. These drawbacks can be vanquish by fabrication of homogeneous catalysts on insoluble and heterogeneous materials, but this method led to a considerable decreasing in their catalytic activity [5]. While,

nanostructured materials have been employed as catalyst directly or catalyst supports for the stabilization of homogeneous catalysts [6, 7]. Nanocatalysts have both advantages of heterogeneous catalysts (stability and recyclability) and homogeneous catalysts (high activity and selectivity) [8]. For example, graphene oxide [9], silica materials [10], polymers [11], ionic liquids [12], carbon nanotubes [13, 14], iron oxide [15, 16], boehmite nanoparticles [17–19], biochar [20, 21], magnetic nanoparticles [22], etc. were reported as nanosupports catalyst. Among, MCM-41 has used in various applications such as catalysis, drug delivery systems, adsorption, extraction, and energy [23]. MCM-41 has unique properties such as high thermal stability, inert in chemical conditions, high surface area, ease and fast of functionalization, nanoscale hexagonal pores, excellent pore volumes (up to 1.3 mL/g), heterogeneous nature and easy separation from the reaction mixture [24]. Also, existence of many Si-OH on its surface allows ease and fast modification of its surface by covalent bands, which allows their applications in the harsh conditions of chemical reactions [25]. Therefore, we investigated 2-Hydroxy-5-nitrobenzaldehyde Schiff-base

✉ Arida Jabbari
   arida_jabbari@yahoo.com

✉ Mohsen Nikoorazm
   e_nikoorazm@yahoo.com

1   Department Of Chemistry, Qeshm Branch, Islamic Azad University, Qeshm, Iran

2   Department of Chemistry, Ilam University, P.O. Box 69315516, Ilam, Iran
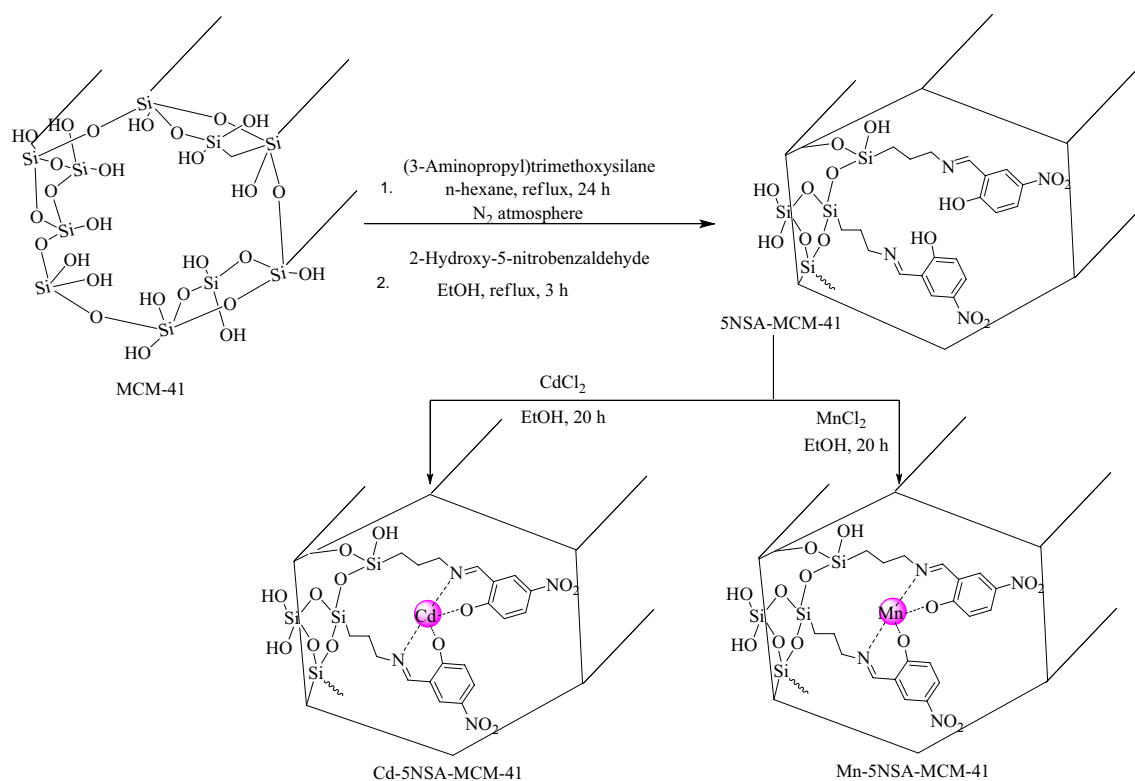
Scheme 1 Synthesis of Cd-5NSA-MCM-41 and Mn-5NSA-MCM-41

complexes of cadmium and manganese on MCM-41 (Cd-5NSA-MCM-41 and Co-5NSA-MCM-41) as efficient, stable and reusable nanocatalysts in the selective oxidation of sulfides using H_2O_2 as oxidant. Because sulfoxide derivatives are effective in the various fields such as synthesis of drugs, natural products, germicides, enzymes activation, and in medicinal chemistry such as antifungal, antibacterial, anti-ulcer, and anti-atherosclerotic agents [26–32]. For example, allicin, modafinal, garlicnin L-1, garlicnin B-2, sulfindac, omeprazole, rabeprazole, esomeprazole and lansoprazole are several types of the sulfoxide derivatives with pharmaceutical and biological activities [27–35].

2 Experimental section

2.1 Materials and instruments

Chemical materials (which were used for the synthesis of catalysts or oxidation of sulfides) were purchased from Aldrich, Merck or Fluka companies. The solvents were purchased from Merck or Iranian companies and used without further purification.

Thermogravimetric analysis (TGA) of the MCM-41, modified MCM-41 and both catalysts were recorded under air atmosphere by a NETZSCH STA 449F3 Thermal

Analysis device. Powder XRD patterns of the MCM-41, modified MCM-41, both catalysts and recovered catalysts were obtained by PW1730 instrument from Philips Company. The exact contents of manganese in Mn-5NSA-MCM-41 and cadmium in Cd-5NSA-MCM-41 were measured by atomic absorption spectroscopy (AAS) analysis using 400p-novAA instrument from Analytik Jena Company. FT-IR spectra of the MCM-41, modified MCM-41, both catalysts and recovered catalysts were recorded with KBr pellets using VRTEX70 model Bruker FT-IR spectrometer. Nitrogen adsorption isotherms of the MCM-41, modified MCM-41 and both catalysts were obtained by a standard gas manifold at 77 K using BELSORP MINI II device. In addition, the catalysts samples were degassed at 120 °C for 2 h using BEL PREP VAC II device before analysis.

2.2 Synthesis of the catalysts

The modified MCM-41 (MCM-41-nPr-NH$_2$) was synthesized according to reported route in Scheme 1 [36]. In order to synthesis of 2-Hydroxy-5-nitrobenzaldehyde Schiff-base ligand on MCM-41 (5NSA-MCM-41), MCM-41-nPr-NH$_2$ (1 g) was refluxed with 2-Hydroxy-5-nitrobenzaldehyde for 3 h in ethanol (EtOH). The obtained solid (5NSA-MCM-41) was isolated by simple filtration, washed with EtOH and dried at room temperature. Finally, 5NSA-MCM-41 (1 g)

was dispersed in EtOH, and then manganese(II) chloride or cadmium(II) chloride was added individually to the mixture and was stirred for 20 h at room temperature. The obtained catalysts (Mn-5NSA-MCM-41 and Cd-5NSA-MCM-41) were filtered, washed and dried at 60 °C (Scheme 1).

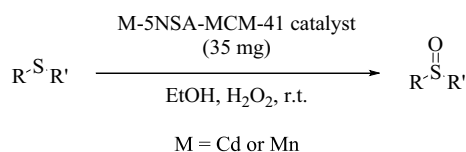## 2.3 General procedure for the oxidation of sulfides to sulfoxides

Mn-5NSA-MCM-41 (0.035 g) or Cd-5NSA-MCM-41 (0.035 g) was added to a solution of 1 mmol of sulfide, 4 mL of ethanol and 7 mmol of H_2O_2. The reaction mixture was stirred at room temperature and the progress of the reaction was controlled by thin-layer chromatography (TLC). In the end of the reaction, the catalyst was separated by filtration and sulfoxide products were extracted by ethyl acetate. The organic solvents were dried over anhydrous sodium sulfate (Na_2SO_4). Then, the organic solvent was evaporated and pure products were obtained in high yields (Scheme 2).
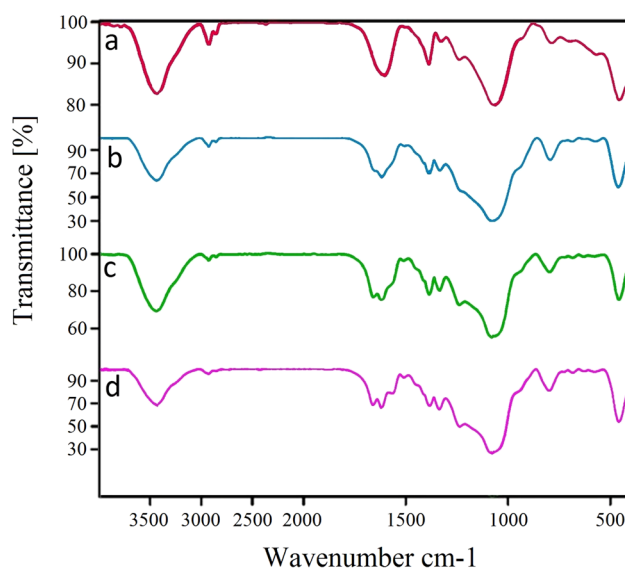
3 Results and discussion

3.1 Characterization of the catalysts

Mn-5NSA-MCM-41 and Cd-5NSA-MCM-41 were characterized by N_2 adsorption–desorption isotherms, Fourier transform infrared spectroscopy (FT-IR), atomic absorption spectroscopy (AAS), X-ray diffraction (XRD), and thermogravimetric analysis (TGA) techniques.

FT-IR spectra of MCM-41-nPr-NH$_2$ (spectrum a), 5NSA-MCM-41 (spectrum b), Mn-5NSA-MCM-41 (spectrum c) and recovered Mn-5NSA-MCM-41 (spectrum d) are shown in Fig. 1. The strong bands about 457, 809, and 1080 cm^{-1} in FT-IR spectra are corresponded to the Si–O–Si vibrations [9]. The broad band above 3000 cm^{-1} in the FT-IR spectra is related to the vibrations of silanol groups [25]. The several weak bands around 3000 cm^{-1} in the FT-IR spectra are related to the vibrations of aromatic and aliphatic C–H bonds [15]. Functionalization of modified MCM-41 nanoparticles with Schiff-base ligand was confirmed by vibrations of imine (C=N) functional groups that is observed at 1640 cm^{-1} in the FT-IR spectrum of 5NSA-MCM-41 and it overlapped with 1618 cm^{-1} band [37]. This peak was shifted to lower


Fig. 1 FT-IR spectra of (**a**) MCM-41-nPr-NH$_2$, (**b**) 5NSA-MCM-41, (**c**) Mn-5NSA-MCM-41 and (**d**) recovered Mn-5NSA-MCM-41

frequency in the FT-IR spectrum of Mn-5NSA-MCM-41, which indicate the loading of metal and successful formation of Schiff-base complex on the modified MCM-41. Also, vibrations of nitro groups (NO$_2$) are observed at 1633 cm^{-1} in the FT-IR spectrum of 5NSA-MCM-41. This peak is observed in the FT-IR spectrum of Mn-5NSA-MCM-41 without any change, which shows that the nitro group does not participate in the formation of the complex.

The TGA analysis of MCM-41, MCM-41-nPr-NH$_2$, 5NSA-MCM-41, Mn-5NSA-MCM-41 (Fig. 2) and Cd-5NSA-MCM-41 (Fig. 2) are indicated the several mass losses from 30 to 800 °C. First of the mass loss is shown at lower than 126 °C, which is related to the desorbed of
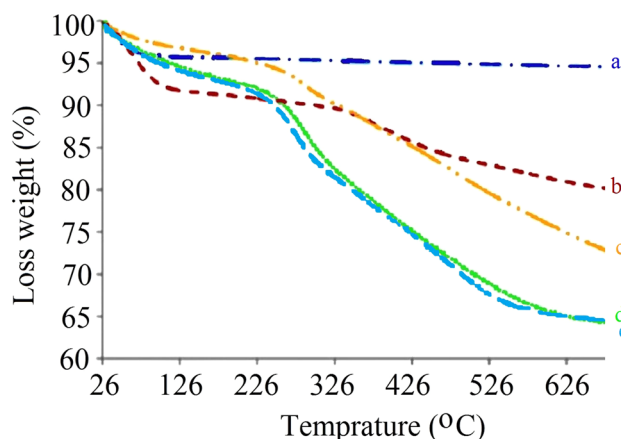
Fig. 2 TGA diagrams of MCM-41 (**a**), MCM-41-nPr-NH$_2$ (**b**), 5NSA-MCM-41 (**c**), Mn-5NSA-MCM-41 (**d**) and Cd-5NSA-MCM-41 (**e**)

Scheme 2 Oxidation of sulfide derivatives to sulfoxide derivatives in the presence of M-5NSA-MCM-41 (M = Cd or Mn)

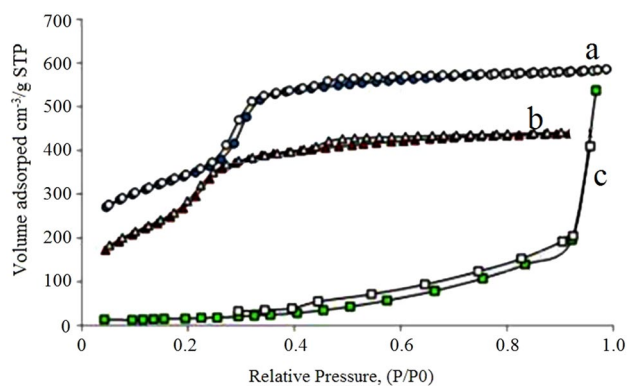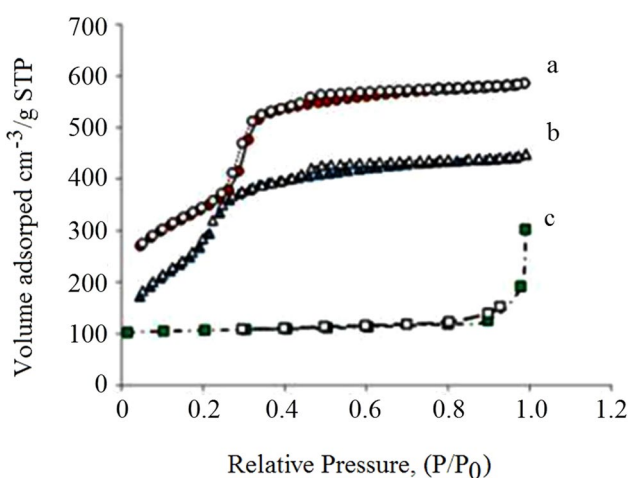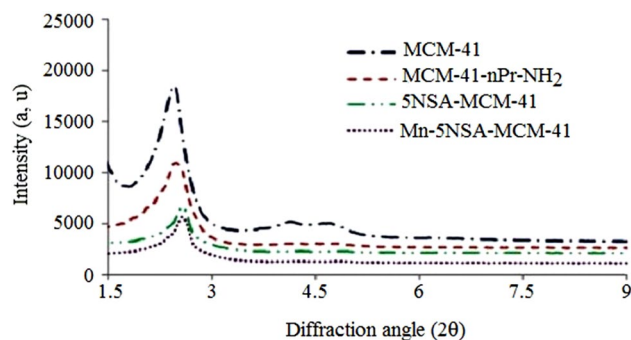**Fig. 3** N$_2$ adsorption–desorption isotherms of MCM-41 (**a**), MCM-41-nPr-NH$_2$ (**b**) and Mn-5NSA-MCM-41 (**c**)

Table 1 Textural properties of MCM-41, MCM-41-nPr-NH$_2$, Mn-5NSA-MCM-41 and Cd-5NSA-MCM-41.

Entry	Sample	S_{BET} (m^2/g)	Pore diameter (nm)	Pore volume (cm^{3}g^{-1})
1	MCM-41	986.16	3.65	0.711
2	MCM-41-nPr-NH$_2$	694.98	3.3	0.340
3	Mn-5NSA-MCM-41	97.33	1.63	0.102
4	Cd-5NSA-MCM-41	31.24	1.2	0.130

Fig. 5 XRD patterns of MCM-41, MCM-41-nPr-NH$_2$, 5NSA-MCM-41, and Mn-5NSA-MCM-41

Fig. 4 N$_2$ adsorption–desorption isotherms of MCM-41 (**a**), MCM-41-nPr-NH$_2$ (**b**) and Cd-5NSA-MCM-41 (**c**)

solvents [17]. The second of the weight loss corresponded to the decomposition of organic moieties (Schiff-base ligand and (3-aminopropyl)triethoxysilane) on the surface of MCM-41, which indicated between 250 and 650 °C [35]. The TGA diagram of MCM-41-nPr-NH$_2$ shows lower weight loss than 5NSA-MCM-41 and Mn-5NSA-MCM-41, because it contains only (3-aminopropyl)triethoxysilane, while 5NSA-MCM-41 and Mn-5NSA-MCM-41 contain Schiff-base ligand more than (3-aminopropyl)triethoxysilane. The TGA diagram of Cd-5NSA-MCM-41 (Fig. 2) is similar to Mn-5NSA-MCM-41 and the weight loss is almost equal to Mn-5NSA-MCM-41.

The N$_2$ adsorption-desorption isotherms of MCM-41, MCM-41-nPr-NH$_2$, Mn-5NSA-MCM-41 (Fig. 3) and Cd-5NSA-MCM-41 (Fig. 4) are shown in Figs. 3 and 4. Also, the obtained results of this analysis are summarized in Table 1. Based on Brunauer-Emmett-Teller (BET), the BET surface area of Mn-5NSA-MCM-41 and Cd-5NSA-MCM-41

are 97.33 m^2/g and 31.24 m^2/g respectively (Table 1, entries 3 and 4). The pore volumes of Mn-5NSA-MCM-41 and Cd-5NSA-MCM-41 are 0.102 cm^3/g and 0.13 cm^3/g respectively. The pore diameters of Mn-5NSA-MCM-41 and Cd-5NSA-MCM-41 are 1.63 nm and 1.2 nm respectively. BET surface area, pore volumes and pore diameters of MCM-41-nPr-NH$_2$ are 694.98 m^2/g, 0.34 cm^3/g and 3.3 nm respectively (Table 1, entry 2). BET surface area, pore volumes and pore diameters of MCM-41 are 986.16 m^2/g, 0.711 cm^3/g and 3.65 nm respectively (Table 1, entry 1). Textural properties of MCM-41 are higher than MCM-41-nPr-NH$_2$, Mn-5NSA-MCM-41 and Cd-5NSA-MCM-41, which is due to the grafting of organic layers and Schiff-base complexes into channels of MCM-41 nanoparticles.

The small angle powder XRD patterns of MCM-41, MCM-41-nPr-NH$_2$, 5NSA-MCM-41, and Mn-5NSA-MCM-41 are shown in Fig. 5. The low angle XRD pattern of Mn-5NSA-MCM-41 shows the peak about $2\theta = 2.6°$ (related to 1 0 0 reflections) and also two weak peaks at $2\theta = 4.3°$ (related to 1 1 0 reflections) and 5.2° (related to 2 0 0 reflections). All the obtained results are in good agreement with hexagonal unit cell of channels of MCM-41 [24]. The decreasing intensity of the peaks in the XRD pattern of Mn-5NSA-MCM-41 is due to immobilization of organic layers and manganese complex in the MCM-41 channels [38]. As we know, the greater the amount of compounds stabilized on MCM-41 channels led to greater decreasing in the intensity

of XRD peaks. The decreasing in intensity of peaks in the XRD pattern of Mn-5NSA-MCM-41 is more than MCM-41-nPr-NH$_2$ and 5NSA-MCM-41, which shows that Schiff-base complex of Mn is well stabilized on MCM-41 [39].

3.2 Catalytic application of the catalysts

Catalytic application of Mn-5NSA-MCM-41 and Cd-5NSA-MCM-41 were investigated in the selective and mild oxidation of sulfides to sulfoxides (Schemes 2). The optimum conditions for the oxidation of sulfide derivatives to sulfoxide derivatives were obtained in the oxidation of dibenzyl sulfide as model reaction (Tables 2 and 3). The oxidation of dibenzyl sulfide was studied in the presence of various amounts of Mn-5NSA-MCM-41 (Table 2, entries 1–5) or Cd-5NSA-MCM-41 (Table 3, entries 1–5), different solvents (Tables 2 and 3, entries 7–15) and various amounts of H$_2$O$_2$ as oxidant (Tables 2 and 3, entries 5–7). The best

Table 2 Optimization reaction conditions for the oxidation of dibenzylsulfane in the presence of Mn-5NSA-MCM-41 catalyst

Entry	Amount of catalyst (mg)	Amount of H$_2$O$_2$ (mmol)	Solvent	Time (h)	Yield (%)[a]
1	10	5	Ethanol	11	90
2	15	5	Ethanol	10	92
3	20	5	Ethanol	5	97
4	25	5	Ethanol	5	98
5	35	5	Ethanol	5	99
6	35	7	Ethanol	4	99
7	35	3	Ethanol	9	91
8	35	7	Ethyl acetate	7	90
9	35	7	n-hexane	42	61
10	35	7	Acetone	24	89
11	35	7	Acetonitrile	7	82
12	35	7	H$_2$O	40	10
13	35	7	Chloroform	7	86
14	35	7	Dichloromethane	7	96
15	35	7	Solvent free	10	Trace

[a] Isolated yield

Table 3 Optimization reaction conditions for the oxidation of dibenzylsulfane in the presence of Cd-5NSA-MCM-41 catalyst

| Entry	Amount of catalyst (mg)	Amount of H$_2$O$_2$ (mmol)	Solvent	Time (h)	Yield (%)[a]
1	10	5	Ethanol	8	83
2	15	5	Ethanol	7	87
3	20	5	Ethanol	5	90
4	25	5	Ethanol	4	92
5	35	5	Ethanol	3	92
6	35	7	Ethanol	2	98
7	35	3	Ethanol	4	88
8	35	7	Ethyl acetate	6	89
9	35	7	n-hexane	41	60
10	35	7	Acetone	24	80
11	35	7	Acetonitrile	6	81
12	35	7	H$_2$O	40	11
13	35	7	Chloroform	6	76
14	35	7	Dichloromethane	6	80
15	35	7	Solvent free	10	Trace

[a] Isolated yield

results were observed in ethanol as solvent using 7 mmol of H_2O_2 in the presence of 35 mg of Mn-5NSA-MCM-41 or Cd-5NSA-MCM-41 at room temperature.

The catalytic application of Mn-5NSA-MCM-41 (Table 4, entries 1–5) and Cd-5NSA-MCM-41 (Table 4, entries 6–10) were investigated in the oxidation of different sulfides (Table 4). Therefore aromatic and aliphatic sulfides were investigated and all products were obtained in excellent yields. Also, heterocyclic sulfides were successfully oxidized to corresponding sulfoxides in the presence of these catalysts. As shown in Scheme 3, these catalysts shows a good selectivity in the oxidation of sulfides to sulfoxides due to mild conditions oxidation.

3.3 Reusability of the catalysts
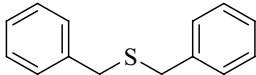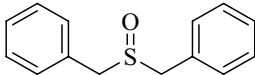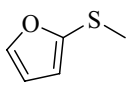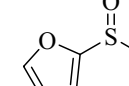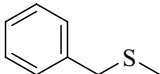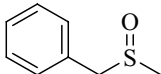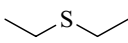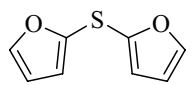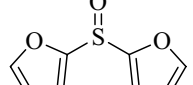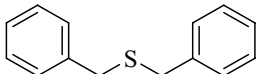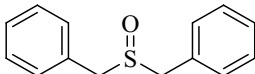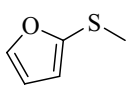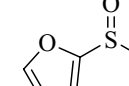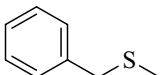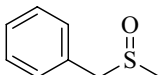
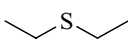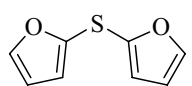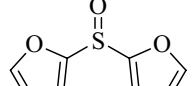The reusability of Mn-5NSA-MCM-41 (Fig. 6a) and Cd-5NSA-MCM-41 (Fig. 6b) catalysts was studied in the
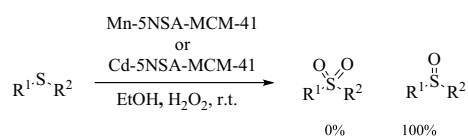
Scheme 3 Selective oxidation of sulfides in the presence of Mn-5NSA-MCM-41 and Cd-5NSA-MCM-41 catalysts

oxidation of dibenzylsulfide. It was found that these catalysts can be easily isolated and successfully reused up to 6 runs. As shown in Fig. 6, these catalysts did not showed any significant change in their activity after reusing. In order to recovering and reusing of the catalysts, the catalysts were separated by centrifugation after each run. The recovered catalysts were washed with ethyl acetate and dried under air atmosphere. Then, dried catalysts were used again in the next cycle without any activation.

Table 4. Synthesis of sulfoxides in the presence of Mn-5NSA-MCM-41and Cd-5NSA-MCM-41 catalysts

Entry	catalyst	Nitrile	product	Time (min)	Yield[a] (%)
1	Mn-5NSA-MCM-41			240	99
2	Mn-5NSA-MCM-41			55	99
3	Mn-5NSA-MCM-41			180	96
4	Mn-5NSA-MCM-41			60	96
5	Mn-5NSA-MCM-41			300	98
6	Cd-5NSA-MCM-41			120	98
7	Cd-5NSA-MCM-41			30	98
8	Cd-5NSA-MCM-41			120	98
9	Cd-5NSA-MCM-41			30	95
10	Cd-5NSA-MCM-41			30	97

[a] Isolated yield
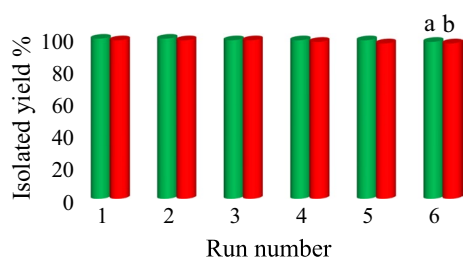
Fig. 6 The reusability of Mn-5NSA-MCM-41 (**a**) and Cd-5NSA-MCM-41 (**b**) in the oxidation of dibenzylsulfide (1 mmol) in the presence of 35 mg of the catalysts and 7 mmol of H_2O_2 in ethanol solvent

3.4 Leaching study of the catalysts

To investigate the heterogeneous nature of the Cd-5NSA-MCM-41 and Mn-5NSA-MCM-41 catalysts, the oxidation of diethyl sulfide was repeated under the optimized conditions in Tables 2 and 3. After completion of the reaction, the catalysts were recovered by filtration. Then, the exact amount of leached metals (Mn or Cd) in the reaction solution was measured by AAS. No significant amount of leached metals (Mn or Cd) was detected in the reaction solution. These results confirm the heterogeneous nature and stability of Cd-5NSA-MCM-41 and Mn-5NSA-MCM-41 catalysts.

Also, to ensure the heterogeneous nature of Cd-5NSA-MCM-41 and Mn-5NSA-MCM-41 catalysts, the exact amount of manganese and cadmium metals were calculated by AAS analysis before and after recovery. The exact amount of manganese in fresh Mn-5NSA-MCM-41 and reused Mn-5NSA-MCM-41 was obtained as 0.0398 mmol/g and 0.0371 mmol/g, respectively. Also, the exact amount of cadmium in fresh Cd-5NSA-MCM-41 and reused Cd-5NSA-MCM-41 was obtained as 0.0755 mmol/g and 0.0742 mmol/g, respectively. These results prove the heterogeneous nature and stability of Cd-5NSA-MCM-41 and Mn-5NSA-MCM-41 catalysts and indicate that no manganese or cadmium leaching occurred in the reaction mixture.

3.5 Characterization of reused catalysts

The recovered Mn-5NSA-MCM-41 and Cd-5NSA-MCM-41 were characterized by XRD (Fig. 7) and FT-IR (Fig. 8) techniques.

The comparison of XRD patterns and FT-IR spectra of recovered and fresh catalysts are shown in Figs. 7 and 8, which any change was not observed after reusing. Good agreement was observed between the XRD patterns and FT-IR spectra of reused and un-reused Mn-5NSA-MCM-41 and Cd-5NSA-MCM-41, which confirms the excellent stability and heterogeneous nature of these catalysts after recycling.
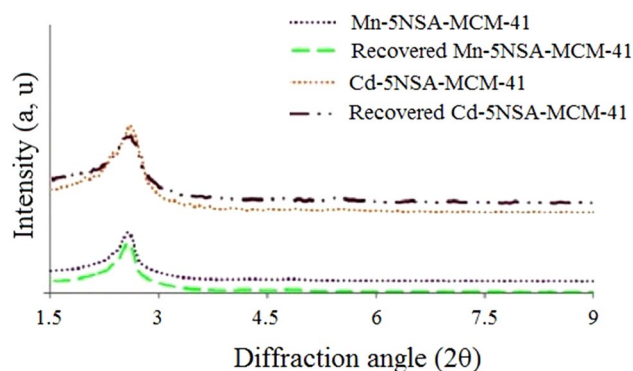
Fig. 7 XRD patterns of Mn-5NSA-MCM-41, reused Mn-5NSA-MCM-41, Cd-5NSA-MCM-41, and reused Cd-5NSA-MCM-41

4 Conclusions

In Conclusion, we synthesized a 2-Hydroxy-5-nitrobenzaldehyde Schiff-base complexes of cadmium and manganese on MCM-41 (Mn-5NSA-MCM-41 and Cd-5NSA-MCM-41). Mn-5NSA-MCM-41 and Cd-5NSA-MCM-41 were characterized by various techniques such as TGA, XRD, BET, AAS and FT-IR. Then, catalytic application of Mn-5NSA-MCM-41 and Cd-5NSA-MCM-41 were studied in the mild and selective oxidation of sulfides to sulfoxides. All products were isolated in high yields. Also, the stability and recyclability of Mn-5NSA-MCM-41 and Cd-5NSA-MCM-41 were described, which shows good recyclability in the oxidation of sulfides. The reused Mn-5NSA-MCM-41 and Cd-5NSA-MCM-41 were characterized by XRD, AAS and FT-IR techniques, which shows a good agreement to the un-used catalyst and confirmed the heterogeneous nature of these catalysts.
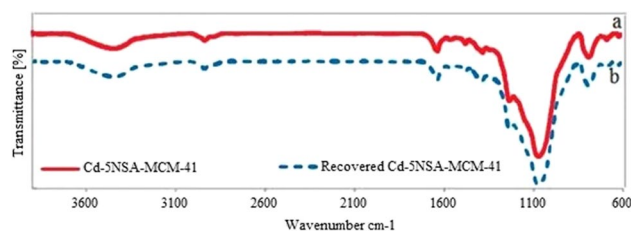
Fig. 8 FT-IR spectra of Mn-5NSA-MCM-41 (**a**), and reused Mn-5NSA-MCM-41 (**b**)

Conflict of interest Authors declare no conflict of interest. All research results are absolutely correct. The article is only this one part that has been submitted to "Journal of Porous Materials".

Consent for publication All authors consent to the publication of this manuscript in "Journal of Porous Materials".

References

1. F. Poovan, V. Chandrashekhar, K. Natte, J. Rajenahally, *Catal* (Technol., Accepted Manuscript, Synergy between homogeneous and heterogeneous catalysis, Sci, 2022). https://doi.org/10.1039/D2CY00232A
2. M. Miceli, P. Frontera, A. Macario, A. Malara, Catalysts **11**, 591 (2021)
3. D.J. Cole-Hamilton, Science **299**, 1702 (2003)
4. V.S. Shende, V.B. Saptal, B.M. Bhanage, Chem. Rec **19**, 1–23 (2019)
5. C.W. Lim, I.S. Lee, Nano Today **5**, 412–434 (2010)
6. D. Astruc, Chem. Rev. **120**, 461–463 (2020)
7. (a) C. Testa, A. Zammataro, A. Pappalardo, G.T. Sfrazzetto, (2019) RSC Adv., 9:27659–27664. (b) P. Moradi, (2022) RSC Adv. 12:33459–33468
8. S.B. Somwanshi, S.B. Somvanshi, P.B. Kharat, (2020) Journal of Physics: Conference Series 1644:012046, doi:https://doi.org/10.1088/1742-6596/1644/1/012046
9. P. Moradi, M. Hajjami, RSC Adv. **11**, 25867–25879 (2021)
10. M. Nikoorazm, B. Tahmasbi, S. Gholami, P. Moradi, Appl. Organomet. Chem. **34**, e5919 (2020)
11. K. Biradha, A. Goswami, R. Moi, Chem. Commun. **56**, 10824–10842 (2020)
12. S.Khazalpour,,M.Yarie,,E. Kianpour, A. Amani, S. Asadabadi, J.Y. Seyf, M. Rezaeivala, S. Azizian, M.A. Zolfigol, J Iran. Chem Soc **17**, 1775–1917 (2020)
13. A.L. Corcho-Valdés, C. Iriarte-Mesa, J. Calzadilla-Maya, Y. Matos-Peralta, L.F. Desdín-García, M. Antuch, (2022) Carbon Composite Catalysts 223–266
14. M. Melchionna, S. Marchesan, M. Prato, P. Fornasiero, Catal. Sci. Technol. **5**, 3859–3875 (2015)
15. M. Nikoorazm, P. Moradi, N. Noori, G. Azadi, J Iran. Chem Soc **18**, 467–478 (2021)
16. B. Atashkar, A. Rostami, H. Gholami, B. Tahmasbi, Res. Chem. Intermed **41**, 3675–3681 (2015)
17. B. Tahmasbi, A. Ghorbani-Choghamarani, P. Moradi, New. J. Chem. **44**, 3717–3727 (2020)
18. A. Ghorbani-Choghamarani, P. Moradi, B. Tahmasbi, Polyhedron **163**, 98–107 (2019)
19. P. A.Jabbari, M. Moradi, B. Hajjami, Tahmasbi, Sci. Rep. **12**, 11660 (2022)
20. P. Moradi, M. Hajjami, New. J. Chem. **45**, 2981–2994 (2021)
21. P. Moradi, M. Hajjami, B. Tahmasbi, Polyhedron **175**, 114169 (2020)
22. P. Moradi, M. Hajjami, RSC Adv. **12**, 13523–13534 (2022)
23. J.A.S. Costa, R.A. de Jesus, D.O. Santos, J.F. Mano, L.P.C. Romão, C.M. Paranhos, Microporous Mesoporous Mater **291**, 109698 (2020)
24. M. Nikoorazm, P. Moradi, N. Noori, J. Porous Mater. **27**, 1159–1169 (2020)
25. M. Nikoorazm, A. Ghorbani–Choghamaranai, M. Khanmoradi, P. Moradi, J. Porous Mater. **25**, 1831–1842 (2018)
26. L. Shiri, B. Tahmasbi, Phosphorus Sulfur Silicon Relat. Elem. **192**, 53–57 (2017)
27. C. Liu, Synth. Commun. **51**, 2237–2264 (2021)
28. A. Ghorbani-Choghamarani, G. Azadi, B. Tahmasbi, M. Hadizadeh-Hafshejani, Z. Abdi, Phosphorus Sulfur Silicon Relat. Elem. **189**, 433–439 (2014)
29. A. Rezaei, A. Ghorbani-Choghamarani, B. Tahmasbi, (2022) Catal. Lett. https://doi.org/10.1007/s10562-022-04135-8
30. M. Azizi, A. Maleki, F. Hakimpoor, R. Ghalavand, A. Garavand, Catal. Lett. **147**, 2173–2177 (2017)
31. A. Maleki, R. Rahimi, S. Maleki, Environ. Chem. Lett. **14**, 195–199 (2016)
32. S.H. Mansourian, S. Shahhosseini, A. Maleki, J. Ind. Eng. Chem. **80**, 576–589 (2019)
33. M.M.D. Pramanik, N. Rastogi, Chem. Commun. **52**, 8557–8560 (2016)
34. K.G.M. Koua, V.M. Dong, Org. Biomol. Chem. **13**, 5844–5847 (2015)
35. A. Ghorbani-Choghamarani, P. Moradi, B. Tahmasbi, J Iran. Chem Soc **16**, 511–521 (2019)
36. (a) T. Kikhavani, P. Moradi, M. Mashari-Karir, J. Naji, (2022) Appl. Organometal. Chem. 36:e6895. (b) M. Nikoorazm, A. Ghorbani–Choghamarani, A. Panahi, B. Tahmasbi, N. Noori, (2018) J. Iran. Chem. Soc. 15:181–189
37. A. Mahdian, M. Hatefi Ardakani, E. Heydari-Bafrooei, S. Saeednia, Appl. Organomet. Chem. **35**, e6170 (2021)
38. M. Nikoorazm, Z. Rezaei, B. Tahmasbi, J. Porous Mater. **27**, 671–689 (2020)
39. B. Tahmasbi, M. Nikoorazm, P. Moradi, Y. Abbasi Tyula, RSC Adv. **12**, 34303–34317 (2022)